

# Nitroxide Spin–Relaxation over the Entire Motional Range

Marco Bonora, Soraya Pornsuwan, and Sunil Saxena\*

Department of Chemistry, University of Pittsburgh, Pittsburgh, Pennsylvania 15260

Received: August 30, 2003; In Final Form: September 5, 2003

Homogeneous line widths, characterized by the phase memory time,  $T_m$ , of a nitroxide spin-labeled peptide, were measured over the entire motional range ( $\sim 10^{-10}$ – $10^{-4}$  s at the spectrometer resonance frequency of 9.7 GHz) using spin–echo correlated spectroscopy (SECSY) ESR. Phase memory times as short as 20 ns could be determined by using schemes designed to minimize the effects of pulse ring-down. Experimental  $T_m$  versus temperature curve (from 192 to 310 K) clearly resolves the  $T_m$  minimum, which provides great sensitivity to the details of molecular dynamics.

## Introduction

In recent years, there has been a significant development of two-dimensional (2D) pulsed methods in electron spin resonance (ESR).<sup>1</sup> These 2D Fourier transform (FT) ESR methods provide improved sensitivity to reorientational dynamics<sup>2</sup> and large interspin distances ( $\sim 15$ – $70$  Å).<sup>3</sup> However, experimental challenges have limited their usefulness when phase memory times,  $T_m$ , become small.

The ESR spectral extents from nitroxides can become as large as 200–250 MHz.<sup>4</sup> To excite this large bandwidth, short ( $\sim 4$ – $6$  ns) and high power ( $\sim$  kW) pulses are required. The ESR signal, on the other hand, is weak ( $\sim$  nW) and decays away rapidly (10–100 ns). The initial, intense part of the time-decaying ESR signal is swamped by the ring-down of the pulse, creating a dead time. Therefore, FT-ESR signals can only be obtained when the phase memory time of the sample is large. For nitroxides,  $T_m$  decreases with temperature in the fast motional regime ( $T_m \propto \tau_R^{-1}$ , where  $\tau_R$  is the rotational correlation time), goes through a minimum, and then increases as temperature decreases in the slow motional regime ( $T_m \propto \tau_R^\alpha$ ,  $1 \leq \alpha \leq 0.5$ ).<sup>5</sup> Resolving dynamics using FT-ESR when temperature is close to the  $T_m$  minimum has been very difficult.

## Experimental Section

**Sample Preparation.** A peptide CPPPPC (C = cysteine and P = proline) was synthesized at the peptide facility of the University of Pittsburgh and was spin-labeled on the cysteines with methanethiosulfonate (MTSSL) procured from Toronto Research Chemicals Inc. A  $5 \times 10^{-4}$  M solution of the labeled peptide in 70% glycerol, 15% 2,2,2-trifluoroethanol, and 15% water buffered (pH 7.2) with MOPS [3-(N-Morpholino) Propane-Sulfonic Acid] was prepared. The sample was degassed using several freeze–pump–thaw cycles to a final pressure of  $4 \times 10^{-5}$  Torr and then flame-sealed.

**ESR Spectroscopy.** ESR experiments were performed using a Bruker EleXsys E580 CW/FT X-band ESR spectrometer equipped with a Bruker ER 4118X-MS3 X-band split ring resonator. Continuous wave (CW) ESR spectra were recorded with a quality factor,  $Q$ , of about 1000, a field-sweep of 200 G, and a modulation amplitude of 1.0 G. The two pulse correlated spectroscopy (COSY-ESR) experiments were obtained with a

resonator  $Q \leq 100$  and an ASE TWTA with an output power of 1 kW. The length of the  $\pi/2$  pulse was 6 ns. The dead time in  $t_1$  was 8 ns. Typically, 32–128 points were collected in  $t_1$  with a step size of 2 or 4 ns. In  $t_2$ , 256 points with a step size of 4 ns were collected. The repetition rate was 5–10 kHz and the number of averages ranged from 500 to 150 K. The COSY-ESR signal was obtained using the usual phase cycle.<sup>1a,b</sup>

A short dead time in  $t_2$  of 28–32 ns was achieved by a combination of two approaches that produce partial cancellation of ring-down artifacts. First, the phase cycle was divided into eight pairs. It was then implemented such that the signal from the second step, in each pair, subtracts from the first.<sup>2a</sup> Second, when the signal becomes very weak (i.e., near the  $T_m$  minimum), an off-resonance signal is subtracted from the on-resonance signal after each step of the phase cycle. This strategy allows a reduction of dead time by as much as 20 ns (i.e., from  $\sim 50$  ns to  $\sim 30$  ns).

The SECSY-ESR spectra are shown in a magnitude mode. The line shape along  $f_2$  is similar to the absorption mode of CW-ESR but is slightly modified by the presence of finite dead times and by the finite coverage of the microwave pulse. The effect of the dead times on the analysis is naturally included in the simulations.<sup>6,7</sup> The effects of finite coverage may be corrected for in the experimental spectra.<sup>2a</sup> However, our analysis focuses on the central component where these effects are minor.

**Simulations.** Spectral simulations were performed using the 2D FT-ESR simulation package NL2DR<sup>6,7</sup> modified to run on a LINUX based computer. A basis set (3% pruning tolerance) was calculated using a minimum truncation set<sup>6,8</sup> of  $L_{\max}^e = 32$ ,  $L_{\max}^0 = 17$ ,  $K_{\max} = 6$ , and  $M_{\max} = 2$ . The magnetic parameters used were  $g_{xx} = 2.0086$ ,  $g_{yy} = 2.0064$ ,  $g_{zz} = 2.0032$ ,  $A_{xx} = A_{yy} = 6.23$  G,  $A_{zz} = 35.7$  G. Theoretical SECSY spectra were calculated for two commonly used models. The first is the model of anisotropic Brownian diffusion<sup>4</sup> while the second is the microscopic order macroscopic disorder (MOMD)<sup>9</sup> model. For each model, axially symmetric rotational rates were used with the anisotropy factor  $N = (R_{\parallel}/R_{\perp}) = 10$ . The simulations were performed as a function of  $\bar{R} = \sqrt[3]{R_{\parallel}R_{\perp}^2}$  and the rotational correlation time,  $\tau_R$ , was determined as  $6\tau_R = 1/\bar{R}$ . A Gaussian inhomogeneous broadening of 1.0 G was used. In the MOMD model, the nitroxide experiences an ordering potential, which was expressed in terms of generalized spherical harmonics as

\* Address correspondence to this author. E-mail: sksaxena@pitt.edu.

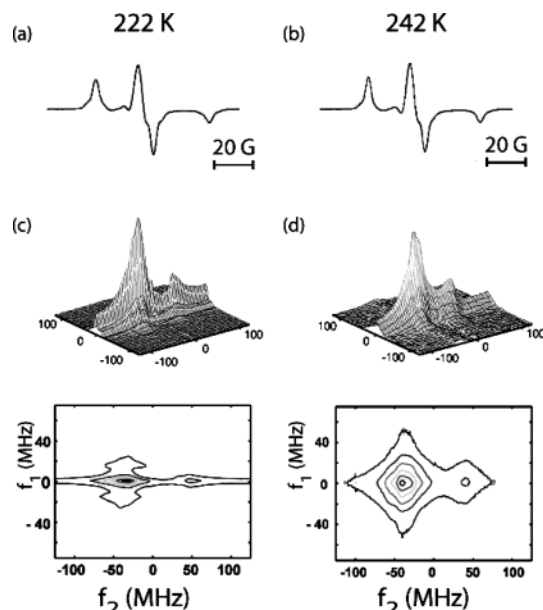


**Figure 1.** Continuous wave ESR spectra for the nitroxide spin-labeled poly-proline peptide are shown at temperatures of (a) 222 K and (b) 242 K. The SECSY-ESR spectra at 222 and 242 K are shown in (c) and (d), respectively, in stack and contour formats. Change in slow-reorientational motion because of change in temperature cannot be resolved in CW-ESR (cf. Figure 1a versus 1b) whereas it leads to dramatic changes in homogeneous line shapes (i.e., the spectrum along  $f_1$ ) in the SECSY-ESR spectra.

$-U/k_B T = \epsilon^2_0 D^2_{00}(\Omega)$ . The coefficient  $\epsilon^2_0$  was kept at 1.0 for all correlation times, although it can be temperature dependent in general. For the MOMD model, the spectra were summed over 10 orientations.

## Results and Discussion

By minimizing ring-down artifacts (cf. Experimental Section), the dead time in  $t_2$  was reduced by as much as 20 ns (i.e., from  $\sim 50$  to  $\sim 30$  ns). For  $T_m \sim 20$  ns, this reduction leads to an increase in detectable echo signal by as much as a factor of 10, making 2D FT-ESR feasible. With the improved dead time, COSY-ESR data were obtained over the entire motional range for the first time on a commercial pulse spectrometer. Such results have been previously obtained only with the help of a home-built spectrometer operating at 17 GHz and the use of 2D FT-ELDOR.<sup>1e,2c,10</sup>

A shearing transform<sup>6</sup> on the “echolike”  $Sc$ -<sup>2,4,6</sup> signal converts these data into the SECSY format. Representative CW-ESR and SECSY spectra are shown in Figure 1 at 222 and 242 K. The line shape along  $f_2$  in the SECSY spectrum is equivalent to that obtained in CW-ESR. The  $f_1$  dimension provides the homogeneous line shape, characterized by the phase memory time  $T_m$ , leading to improved sensitivity to slow dynamics.<sup>11</sup> Despite the change in temperature by 20 K, the CW-ESR spectra are practically identical, indicating weak sensitivity to dynamics in this very slow motional regime. On the other hand, the  $f_1$  dimension in the SECSY spectra shows clear changes—the line width changes by a factor of 4 (cf. Figure 1c versus 1d).

The  $T_m$ , in general, depends on the  $f_2$  and a full analysis of this variation is sensitive to details of molecular dynamics.<sup>11</sup> We show that the resolution of the  $T_m$  minimum provides an easy distinction between the dynamical models commonly used to interpret ESR spectra. In Figure 2, the  $T_m$  for the central component is shown as a function of inverse temperature. Each phase memory time was obtained by extracting a slice parallel

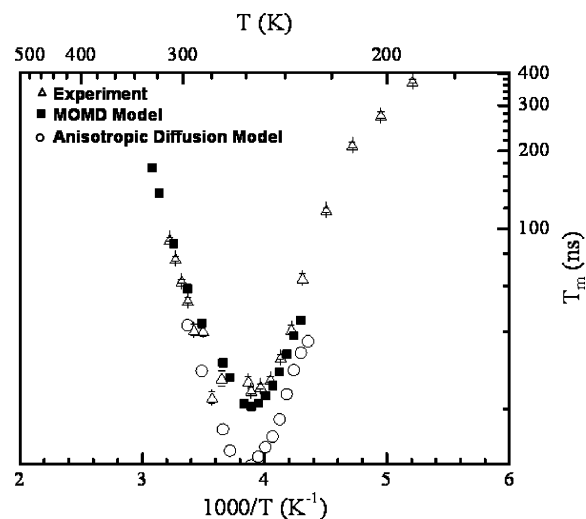


**Figure 2.** Experimental phase memory times plotted on a logarithmic scale versus inverse temperature for the central component (triangles). Theoretical  $T_m$ 's are shown for two models of dynamics: an anisotropic Brownian diffusion model (circles) and the microscopic order macroscopic disorder (MOMD) model (filled squares). The  $T_m$  versus  $1/T$  curve is sensitive to details of microscopic dynamics.

to  $f_1$  and determining the full width at half-height. To quantitatively analyze the data, SECSY spectra for a series of rotational correlation times,  $\tau_R$ , were calculated using spectral simulations based on the stochastic Liouville equation.<sup>5–8</sup> These spectra were simulated for several models of microscopic dynamics (see Experimental Section).

Theoretical  $T_m$  values were obtained for each  $\tau_R$  by examining the line shape along  $f_1$  as described above. To fit theoretical  $T_m$  values (obtained versus  $\tau_R$ ) to experimental data (obtained versus temperature,  $T$ ), a relationship between  $\tau_R$  and  $T$  is needed. The correlation time is proportional to  $\eta/T$  where  $\eta$  is the viscosity of the solution and an Arrhenius-type relationship is usually used to relate  $\tau_R$  and  $T$ .<sup>4,5a</sup>

$$\ln(\tau_R/A) = E_a/RT \quad (1)$$

where  $A = 8.4 \times 10^{-16}$  s and  $E_a = 7.9$  kcal/mol. The activation energy,  $E_a$ , for this system was determined from experimental slow motional data, as described before.<sup>4</sup> Within experimental uncertainties, this value is consistent with earlier results on an analogous system in glycerol–water–trifluoroethanol solvent.<sup>4</sup> The parameter  $A$  was adjusted for best fit. Both parameters serve to shift the theoretical curve parallel to the  $1/T$  axis.

The model of anisotropic Brownian diffusion qualitatively predicts a similar curve but leads to reduced  $T_m$  minimum. The model of anisotropic diffusion in a reorientational potential (i.e., the MOMD model) provides a better fit to the data. This model is intuitively pleasing for this system—the nitroxide experiences an ordering potential, because of the peptide chain, which restricts its amplitude of rotational motion. While these simulations do not include the small effects of dipolar relaxation, this comparison does demonstrate the sensitivity of  $T_m$ 's near the minimum to details of motion.

## Conclusions

We demonstrate the feasibility of resolving reorientational dynamics over the entire motional range in tethered nitroxides using FT-ESR even on commercial spectrometers. The resolution of the  $T_m$  minimum allows easy distinction between commonly used models of dynamics. This opens up the

possibility of using 2D ESR for the study of spin-labeled proteins, which is of significant current interest.<sup>12</sup>

Acknowledgment is made to the donors of the Petroleum Research Fund, administered by the American Chemical Society and the Central Research Development Fund, University of Pittsburgh for partial support of this research. Helpful discussions with Drs. Ralph Weber and Dave Schneider are gratefully acknowledged.

**Supporting Information Available:** Details about the phase cycle and about the temperature dependence of SECSY-ESR and CW-ESR line widths are provided. This material is available free of charge via the Internet at <http://pubs.acs.org>.

## References and Notes

- (1) (a) Gorcester, J.; Freed, J. H. *J. Chem. Phys.* **1988**, *88*, 4678. (b) Patyal, B. R.; Crepeau, R. H.; Gamliel, D.; Freed, J. H. *Chem. Phys. Lett.* **1990**, *175*, 445. (c) Miick, S. M.; Millhauser, G. L. *J. Magn. Reson., Ser. B* **1994**, *104*, 81. (d) Milov, A. D.; Tsvetkov, Yu. D.; Formaggio, F.; Crisma, M.; Toniolo, C.; Raap, J. *J. Am. Chem. Soc.* **2000**, *122*, 3843. (e) Borbat, P. P.; Costa-Filho, A. J.; Earle, K. A.; Moscicki, J. K.; Freed, J. H. *Science* **2001**, *291*, 266. (f) Schweiger, A.; Jeschke, G. *Principles of pulse electron paramagnetic resonance*; Oxford University Press: New York, 2001.
- (2) (a) Crepeau, R. H.; Saxena, S.; Lee, S.; Patyal, B. R.; Freed, J. H. *Biophys. J.* **1994**, *66*, 1489. (b) Patyal, B. R.; Crepeau, R. H.; Freed, J. H. *Biophys. J.* **1997**, *73*, 2201. (c) Costa-Filho, A. J.; Shimoyama, Y.; Freed, J. H. *Biophys. J.* **2003**, *84*, 2619.
- (3) (a) Larsen, R. G.; Singel, D. J. *J. Chem. Phys.* **1993**, *98*, 5134. (b) Saxena, S.; Freed, J. H. *J. Chem. Phys.* **1997**, *107*, 1317. (c) Milov, A. D.; Maryasov, A. G.; Tsvetkov, Yu. D.; Raap, J. *Chem. Phys. Lett.* **1999**, *303*, 135. (d) Borbat, P. P.; Freed, J. H. *Chem. Phys. Lett.* **1999**, *313*, 145. (e) Jeschke, G.; Pannier, M.; Godt, A.; Spiess, H. W. *Chem. Phys. Lett.* **2000**, *331*, 243. (f) Pannier, M.; Schädler, V.; Schöps, M.; Wiesner, U.; Jeschke, G.; Spiess, H. W. *Macromolecules* **2000**, *33*, 7812. (g) Milov, A. D.; Tsvetkov, Yu. D.; Formaggio, F.; Crisma, M.; Toniolo, C.; Raap, J. *J. Am. Chem. Soc.* **2001**, *123*, 3784. (h) Borbat, P. P.; Mchaourab, H. S.; Freed, J. H. *J. Am. Chem. Soc.* **2002**, *124*, 5304. (i) Milov, A. D.; Tsvetkov, Yu. D.; Gorbunova, E. Yu.; Mustaeva, L. G.; Ovchinnikova, T. V.; Raap, J. *Biopolymers* **2002**, *64*, 328.
- (4) Saxena, S.; Freed, J. H. *J. Phys. Chem. A* **1997**, *101*, 7998.
- (5) (a) Stillman, A. E.; Schwartz, L. J.; Freed, J. H. *J. Chem. Phys.* **1980**, *73*, 3502. (b) Schwartz, L. J.; Stillman, A. E.; Freed, J. H. *J. Chem. Phys.* **1982**, *77*, 5410.
- (6) Lee, S.; Budil, D. E.; Freed, J. H. *J. Chem. Phys.* **1994**, *101*, 5529.
- (7) Budil, D. E.; Lee, S.; Saxena, S.; Freed, J. H. *J. Magn. Reson., Ser. A* **1996**, *120*, 155.
- (8) Schneider, D. J.; Freed, J. H. In *Advances in Chem. Phys.*; Hirschfelder, J. O., Wyatt, R. E., Coalson, R. D., Eds.; Wiley: New York, 1989; Vol. 63.
- (9) Meirovitch, E.; Nayeem, A.; Freed, J. H. *J. Phys. Chem.* **1984**, *88*, 3454.
- (10) (a) Borbat, P. P.; Crepeau, R. H.; Freed, J. H. *J. Magn. Reson.* **1997**, *127*, 155. (b) Freed, J. H. *Annu. Rev. Phys. Chem.* **2000**, *51*, 655. (c) Costa-Filho, A. J.; Crepeau, R. H.; Borbat, P. P.; Ge, M.; Freed, J. H. *Biophys. J.* **2003**, *84*, 3364.
- (11) Millhauser, G. L.; Freed, J. H. *J. Chem. Phys.* **1984**, *81* (1), 37.
- (12) (a) Altenbach, C.; Marti, T.; Khorana, H. G.; Hubbell, W. L. *Science* **1990**, *248*, 1088. (b) Millhauser, G. L. *Trends Biochem. Sci.* **1992**, *17*, 448. (c) Raucher, D.; Fajer, P. G. *Biochemistry* **1994**, *33*, 11993. (d) Farrens, D. L.; Altenbach, C.; Yang, K.; Hubbell, W. L.; Khorana, H. G. *Science* **1996**, *274*, 768. (e) Poirier, M. A.; Xiao, W.; Macosko, J. C.; Chan, C.; Shin, Y.-K.; Bennett, M. K. *Nat. Struct. Biol.* **1998**, *5*, 765. (f) Polese, A.; Anderson, D. J.; Millhauser, G. L.; Formaggio, F.; Crisma, M.; Marchiori, F.; Toniolo, C. *J. Am. Chem. Soc.* **1999**, *121*, 11071. (g) Merianos, H. J.; Cadieux, N.; Lin, C. H.; Kadner, R. J.; Cafiso, D. S. *Nat. Struct. Biol.* **2000**, *7*, 205. (h) Hubbell, W. L.; Cafiso, D. S.; Altenbach, C. *Nat. Struct. Biol.* **2000**, *7*, 735. (i) Perozo, E.; Cortes, D. M.; Sompornpisut, P.; Kloda, A.; Martinac, B. *Nature* **2002**, *418*, 942.